

FLAT-PLATE PHOTOVOLTAIC ARRAY DESIGN OPTIMIZATION*

R. G. Ross, Jr.**

Jet Propulsion Laboratory, Pasadena, California

SUMMARY

Specific analyses have been conducted in the areas of structural design optimization, optimization of array series/parallel circuit design, thermal design optimization, optimization of environmental protection features, and others. This paper integrates the results from these various studies and draws general conclusions relative to optimal features for future modules. The described analysis is based on minimizing the total photovoltaic system life-cycle energy cost including repair and replacement of failed cells and modules. The conclusions presented provide useful design guidelines for designers of future flat-plate photovoltaic modules.

INTRODUCTION

A comprehensive program of flat-plate solar array design optimization is being carried out as part of the Jet Propulsion Laboratory's Low-cost Solar Array Project. The objective of these studies is to define means of reducing the cost and improving the utility and reliability of photovoltaic flat-plate arrays for the broad spectrum of terrestrial applications. Specific analyses have been conducted in the areas of structural design optimization, optimization of array series/parallel circuit design, thermal design optimization, optimization of environmental protection features, and others.

This paper describes a key analysis which serves to integrate many of these ongoing studies and is based on minimizing the total PV system life-cycle energy cost including repair and replacement of failed cells and modules. This analysis directly integrates array structures costs, panel costs, module costs, replacement strategies, series/paralleling tradeoffs, module size tradeoffs, cell reliability performance, and several other factors.

THE PROBLEM

The primary objective of the described analysis is to provide a means of integrating the results from a variety of diverse flat-plate solar array design

studies and to draw bottom-line conclusions relative to optimum module and array mechanical and electrical circuit configurations. Because of the strong interaction between module size and replacement cost, any analysis of module size is forced to also consider the expected degree and timing of module replacement. This is further tied to the entire question of module reliability, definition of module failure and replacement criteria, and the reliability engineering features, such as series/parallel, by-pass diodes, and redundant solar cell electrical contacts. Looked at the other way around, any analysis for the selection of the optimal reliability engineering features must also consider the costs of replacement, including the size of the modular replacement unit.

To illustrate the nature of the problem consider the selection of the optimum mechanical and electrical configuration for a flat-plate module for a large ground-mounted photovoltaic array. A complete analysis should, as a minimum, address the following interactions:

- Module superstrate (glass) thickness and material cost versus size
- Module efficiency (perimeter area effect and encapsulant transmission) versus size
- Module efficiency loss due to cell mismatch versus circuit configuration
- Module assembly cost versus size and circuit configuration
- Module manufacturing yield cost (larger modules have higher probability of containing faulty parts, but greater circuit redundancy reduces losses associated with faults)
- Module shipping and handling and installation cost versus size
- Support structure cost versus module size and efficiency

* This paper presents the results of one phase of research conducted at the Jet Propulsion Laboratory, California Institute of Technology, for the U.S. Department of Energy, by agreement with the National Aeronautics and Space Administration.

**Engineering Manager, Low-cost Solar Array Project, Energy Technology Engineering Section.

- Field cabling costs versus module size and efficiency
- System power degradation versus electrical circuit reliability as influenced by series/paralleling, by-pass diodes, multiple cell contacts, etc.
- Module life-cycle replacement cost versus module size and system power degradation

Review of the above interactions indicates the complexity of the problem at hand.

APPROACH

The approach utilized to solve the above problem first involves generating parametric data defining the cost/performance dependency associated with each of the bulleted interactions except the last. This work is basically complete and has resulted from a variety of JPL inhouse configuration and series/paralleling studies and power-system/support-structure/maintenance-cost studies conducted by Bechtel Corporation under contract to JPL (1), (2), (3), (4), (5). Details of these results will be examined later in this paper.

The next step in the solution is the construction of an overall cost optimization algorithm based on minimizing the total system life-cycle energy cost including selection of the optimum module replacement strategy. This has been accomplished using a multi-variable optimization program which first repeatedly computes the system life-cycle energy costs using different module replacement strategies until the least-cost strategy is identified. The analysis is then repeated for each alternative system configuration (module size and electrical circuit) to allow selection of the least-cost total system design including the module replacement strategy.

The optimization is formulated by setting the life-cycle benefits equal to the life-cycle costs including module replacement over the life of the plant. In mathematical form the derivation follows this author's previous work (6):

$$\text{Life-cycle benefit} = \sum_{i=0}^{20} RE_1(1+k)^{-i}$$

$$\text{Life-cycle cost} = C_0 + \sum_{i=1}^{20} C_1 M_1 (1+k)^{-i}$$

where:

- R = Cost (worth) of energy assumed constant over the plant lifetime (startup-year \$/kW-hr)
- E₁ = Energy generated in year 1 (kW-hrs)
- C₀ = Initial plant cost (startup-year \$)
- C₁ = Cost per module replacement action (startup-year \$/module)
- M₁ = Number of modules replaced in year 1
- k = Present value discount rate
- 20 = Plant lifetime (years)

The optimum system design is then found by minimizing the breakeven cost of the photovoltaic energy which is given by:

$$R = \frac{C_0 + \sum_{i=1}^{20} C_1 M_1 (1+k)^{-i}}{\sum_{i=0}^{20} E_1 (1+k)^{-i}} \quad (1)$$

Two numerical algorithms have been successfully used to perform the actual minimization at JPL. The first uses a multivariable optimization program written by this author based on the simplex method of Nelder and Mead (7). This program repeatedly evaluates any arbitrary function of n variables and locates the values of the variables where the function is minimum. For the problem at hand the function to be minimized is equation (1) and the n variables are the 20 values of M₁ representing the number of modules replaced in each of the twenty years of the photovoltaic system's life.

The simplex algorithm has the advantage of being able to locate the least-cost replacement strategy independent of its complexity. However, it suffers the disadvantage of converging very slowly. An important finding from the use of this algorithm is that in nearly all cases analyzed the optimum replacement strategy has been either no module replacement at all, or module replacement each time a solar cell fails. In the rare cases where one of these two options has not been optimum, the optimum replacement strategy has always been to fully replace failed modules in the first few years of the system's life, and then to replace no modules in subsequent years.

Based on this finding a second optimization algorithm has been developed based on selecting the least cost of 21 trial replacement strategies. The 21 trial strategies include no replacement at all, and module replacement for each cell that fails during the first through the rth year (r = 1, 20) with no replacement for the balance of the plant's 20-year life. This algorithm works very efficiently and is the one currently being used at JPL.

The remainder of this paper is devoted to implementing this algorithm for the case of large multi-megawatt ground-mounted arrays similar to those that might be used in a large industrial or central station application. Although the number of design alternatives considered has been limited for presentation purposes, the approach is being applied to a much more exhaustive set of alternatives including residential applications as part of the ongoing JPL/LSA Engineering activities.

COST DEPENDENCIES FOR LARGE GROUND-MOUNTED ARRAYS

As a first step in the analysis it is necessary to define the cost/performance dependency associated with each of the important interactions bulleted earlier in this paper. Bechtel Corporation, in their work for JPL, has developed a number of

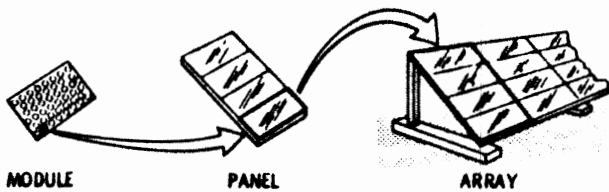


Fig. 1. Definition of array elements

these dependencies for large ground-mounted steel frame arrays.

In their work Bechtel has examined three module sizes (2 x 4 foot, 4 x 4 foot, and 4 x 8 foot) and a number of alternative support-structure configurations. For lowest installed cost their analysis indicates that modules should be factory-mounted and shipped in structural panels which become integral parts of the array structure as shown in Figure 1. Although they found the areal cost of the glass to be the same for each of the three module sizes (because of minimum gauge considerations), the cost of the panel structure was found to be strongly dependent on the module size. On the other hand, the total structural cost was found to vary little between alternative panel sizes and support-structure configurations for a given module size.

Based on this last finding a single frame/support structure configuration and single panel size (8 x 16 foot) is used throughout the remainder of this paper.

Bechtel also developed a variety of installation and replacement cost scenarios. Their least cost scenario, which is adopted in this paper, involves locating the faulty panel in the field and exchanging the panel with a new or rebuilt one. The faulty panel is then returned to a repair station where the faulty module is located within the panel and is replaced with a new module. The rebuilt panel is now ready for reuse in the field. Table I summarizes these cost dependencies.

Also included in Table I is the cost for the photovoltaic module (a glass solar cell sandwich with no frame) including a term referred to as module yield cost. The module yield cost is the amount that must be added to the price of a module to pay for modules scrapped during module final assembly, shipping and installation due to broken cells and other circuit failures. The module failure criteria is based on controlling electrical mismatch in the array and assumes that a module is rejected if its power loss is greater than 10 percent of the average peak power output for all modules. The yield cost value in Table I is for a circuit failure density of 1 per 1000 solar cells, and is dependent on the level of module circuit redundancy. Figure 2 summarizes the yield figures computed for this failure density as a function of module series/paralleling for three sizes of modules (2). Because automated soldering techniques are assumed, no additional module cost is associated with the increased internal series/paralleling.

Table 1. Cost Dependencies for Array Elements

ELEMENT	UNITS (1975 \$)	MODULE SIZE (ft x ft)		
		2 x 4	4 x 4	4 x 8
INITIAL:				
MODULE DIRECT COST	\$/m ²	60	60	60
MODULE YIELD COST*	\$/m ²	0-5	0-8	0-23
• MODULE SUBTOTAL	\$/m ²	60-65	60-68	60-83
PANEL FRAME	\$/m ²	24	18	15
PANEL WIRING	\$/m ²	2-4	2-3	1-2
• PANEL SUBTOTAL	\$/m ²	26-28	20-21	16-17
PANEL INSTALLATION	\$/m ²	1	1	1
INSTALLED ARRAY STRUCT	\$/m ²	22	22	22
• ARRAY TOTAL	\$/m ²	109-116	103-112	99-123
PER REPLACEMENT ACTION:				
FAULT IDENTIFICATION	\$/PANEL	4	4	4
PANEL SUBSTITUTION LABOR	\$/PANEL	21	21	21
MODULE REPLACEMENT LABOR	\$/MOD	12	12	12
REPLACEMENT MODULE PARTS (INC 1% INVENTORY COST)	\$/m ²	61-66	61-69	61-84

*1 CELL FAILURE PER 1000 DURING ASSEMBLY/SHIPPING/INSTALLATION

Another important area of cost dependency involves parameters which alter module or array electrical efficiency. Changing efficiency directly leverages the total quantity of modules and support structure required, and thus directly impacts the initial plant cost. Two efficiency dependencies are important in the present analysis: a) decreased module packing efficiency due to increased border on smaller modules (1), and b) decreased cell mismatch losses associated with high degrees of series/paralleling (3). The effect of these and other system performance dependencies are summarized in Table II.

Except for the module efficiency entries, the majority of the figures in Table II reflect nominal values required in the life-cycle energy cost calculations and have little impact on the relative comparisons which result from the analyses.

ARRAY DEGRADATION VERSUS CIRCUIT REDUNDANCY

The remaining dependency which must be examined is the effect of electrical circuit redundancy on array power degradation resulting from field failures. Before discussing the specifics of this subject it is useful to first introduce some circuit redundancy concepts and nomenclature.

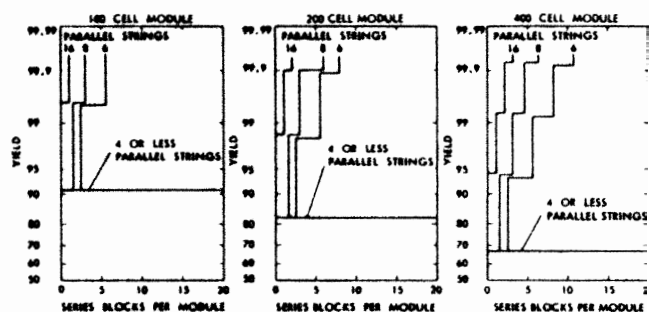


Fig. 2. Module yield versus series paralleling assuming one failure per 1000 cells and module rejection for power loss greater than 10 percent

Table 2. Nominal Life-Cycle Performance Parameters

INITIAL ARRAY EFFICIENCY	MODULE SIZE (ft x ft)		
	2 x 4	4 x 4	4 x 8
ENCAP. CELL EFFICIENCY	0.15	0.15	0.15
NOCT EFFICIENCY	0.92	0.92	0.92
PACKING EFFICIENCY	0.89	0.91	0.93
ARRAY EFFICIENCY SUBTOTAL	0.123	0.126	0.128
BALANCE-OF-PLANT EFFICIENCY			
ELECTRICAL EFFICIENCY	0.92		
MODULE SOILING EFFICIENCY	0.92		
BALANCE-OF-PLANT SUBTOTAL	0.85		
BALANCE-OF-PLANT COSTS (1978)	150 \$/KW		
DISCOUNT RATE (OVER INFLATION)	10%		
ANNUAL INSOLATION	1825 kW-h/m ² /yr		

From a variety of overall photovoltaic system studies including work by Bechtel and others there is good agreement that large centralized power systems will be logically subdivided into a number of individual array subfields in the 2 to 10 megawatt size range (4). It has also been determined that the optimum DC voltage level for a subfield of this size will be somewhere in the 1000 to 2000 volt range so as to control I²R losses in the field wiring and power conditioner (4). Because each solar cell produces an output of approximately 1.0 watt at 0.5 volts, it can be seen that each power conditioner will be fed by an approximately square matrix of from 2 to 10 million individual solar cells.

The first step toward circuit redundancy is generally associated with dividing this large matrix of cells into a number of parallel solar cell networks referred to as "branch circuits." The branch circuits provide convenient points for monitoring array performance and provide an ability to isolate small areas of the total array for maintenance and repair. As shown in Figure 3 each branch circuit may contain a single string of series solar cells or a number of parallel strings interconnected periodically by cross ties. The cross ties divide each branch circuit into a number of "series blocks."

It is the series/paralleling of the individual branch circuits which is key to controlling array degradation. Three parameters are of particular importance--the number of parallel strings, the number of series blocks, and the number of cells per substring within each series block. For any specific branch circuit configuration the sub-string failure density (F_{ss}) can be easily computed from the cell failure density (F_c) and the number of cells per substring (n) using the following statistical equation:

$$F_{ss} = 1 - (1 - F_c)^n \quad (2)$$

During operation of the life-cycle optimization program the cell failure density present in the array at any point in its life is computed by summing the net failures to date due to the assumed

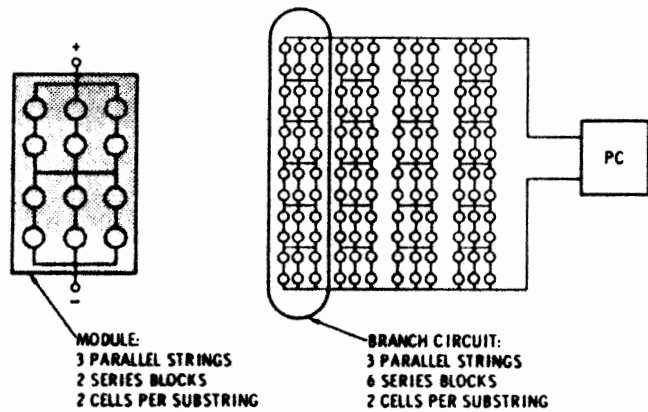


Fig. 3. Series/parallel nomenclature

failure rate together with the effect of module replacements in preceding years. For the analyses which follow the cell failure rate has been set equal to a constant value of one open-circuit cell failure per 10,000 cells per year. This value is felt to be a reasonable expectation for future large scale arrays and is only a factor of two or so better than is currently being experienced in the 25 kW Mead, Nebraska, experiment. A failure rate of 1 per 1000 per year is also examined to indicate the sensitivity of selected results to the failure rate.

A major computational difficulty is the task of computing the array power degradation for each substring failure density level and for the variety of array series/parallel/diode electrical circuit configurations of interest. A major activity at JPL has been addressed to this problem over the last year and has led to the development of an elaborate parametric analysis described in detail in a companion paper (2). The results from this analysis are entered into the life-cycle cost optimization program and are used to compute the system power output each year of its 20-year life based on the net cell failure density that year. An example plot defining the dependence between average branch circuit power loss and substring failure density for series/parallel circuits involving 8 parallel strings and various numbers of series blocks is shown in Figure 4.

To set the stage for the life-cycle analyses which follow in the next section, it is instructive to consider the problem of calculating the expected power degradation for a 1000 volt, large industrial array made up of 8 parallel-string branch circuits as considered in Figure 4. To achieve the 1000 volt nominal operating voltage requires approximately 2400 series solar cells, and thus a branch circuit of 2400 series by eight parallel. If 14 cross ties are incorporated into each branch circuit, there will be 15 series blocks per branch circuit and 2400/15 = 160 cells per substring.

To utilize Figure 4 it is first necessary to compute the expected substring failure density for the time of interest. As an example, the sub-

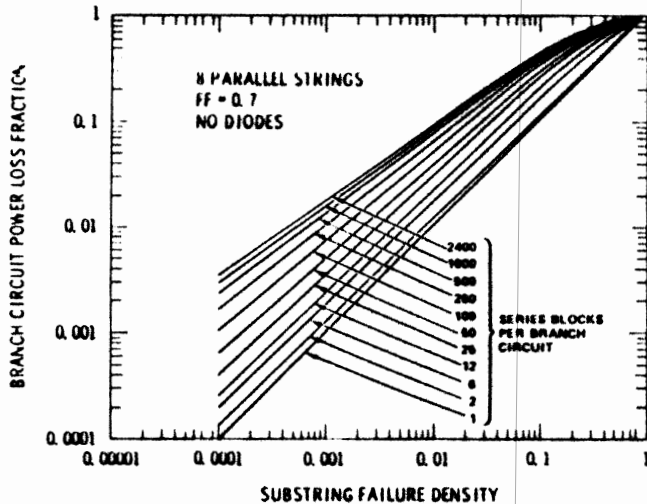


Fig. 4. Power loss relationships for 8-parallel-string branch circuits

string failure density at the end of five years with no module replacements and a constant cell failure rate of 0.0001 per year is found using equation (2) as:

$$F_{SS} = 1 - (1 - 0.0005)^{160} = 0.0769$$

Using this value and interpolating in Figure 4 gives an expected array degradation of approximately 16 percent after 5 years. Figure 5 expands on this result to illustrate the expected degradation in subsequent years and the result of different numbers of series blocks per branch circuit.

LIFE-CYCLE ANALYSIS RESULTS

As an example application, the life-cycle optimization algorithm is now used to calculate the life-cycle cost tradeoffs associated with the previous example which incorporated branch circuits with 8 parallel by 2400 series cells and a uniform cell failure rate of 0.0001 per year. In addition, the analysis is initially focused on the use of 4 by 8 foot modules, each containing 320 solar cells, and with the cost dependencies previously developed in Tables I and II. For these assumptions Figure 6 displays the calculated life-cycle energy costs as a function of the number of series blocks per branch circuit and for two replacement strategies. In the first strategy no module replacement is allowed and it can be seen that the life-cycle costs increase sharply with low numbers of series blocks. This reflects the rapid array degradation exhibited in Figure 5 for these circuit configurations.

For the second curve in Figure 6 modules are replaced each time a solar cell fails during the 20-year life of the plant. This results in no power degradation, but does cause a substantial module replacement-cost contribution. This cost also varies with the number of series blocks due to reductions in module yield costs which occur

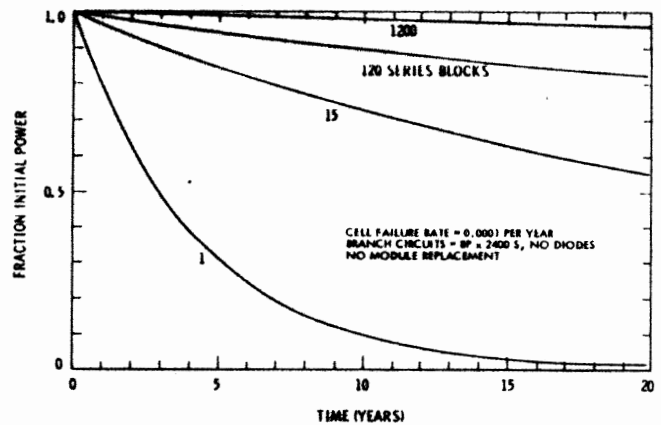


Fig. 5. Array power degradation for 8-parallel-string branch circuits

when module series/paralleling achieves 8 parallel by two or more series blocks. This degree of module series/paralleling is only possible when 120 or more series blocks are used per branch circuit.

As seen in Figure 6 the optimum maintenance strategy depends on the degree of series/paralleling. When low degrees of series/paralleling are used, the least-cost maintenance strategy is to replace the affected module each time a solar cell fails. On the other hand, when a high degree of series/paralleling is used, the least-cost strategy involves no module replacement. Only in a very small region where the two curves cross is a partial-replacement strategy optimum.

In future graphs only the optimum-maintenance (least life-cycle) cost is plotted for each number of series blocks per branch circuit.

When considering Figure 6 it is apparent that the optimum configuration for an array of 4 by 8 foot modules in 8-parallel-string branch circuits is 240 or more series blocks, with no module replace-

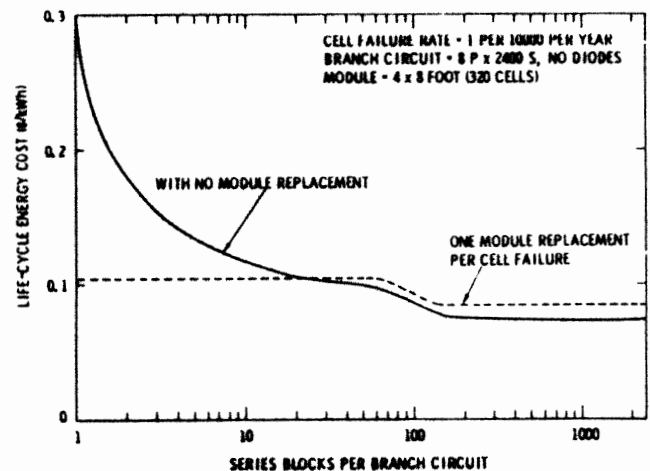


Fig. 6. Life-cycle energy costs for 8-parallel-string branch circuits

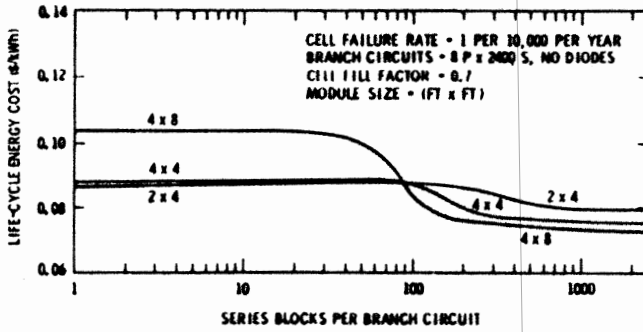


Fig. 7. Minimum life-cycle energy costs for various module sizes

ment. Figure 7 compares this result with similar results for 2 by 4 and 4 by 4 foot modules. As seen in Figure 7 both smaller module sizes result in higher system energy costs because of the higher support structure cost for small modules. Also, the cost reduction due to yield-cost improvements occurs at a higher number of series blocks because of the fewer cells per module.

If, for some reason, a low degree of series/paralleling is utilized together with a full replacement strategy, the smaller modules are preferred over the larger 4 by 8 foot modules. This is because of the higher per unit replacement cost for large modules and the similarly higher yield costs when no module internal series/paralleling can be utilized.

Figure 8 illustrates the key argument against the adoption of this low-series/paralleling, full-replacement strategy by indicating the effect of a higher cell failure rate. As can be seen the low-series/paralleling configurations are much more sensitive to higher than expected failure rates than are the high-series/paralleling configurations.

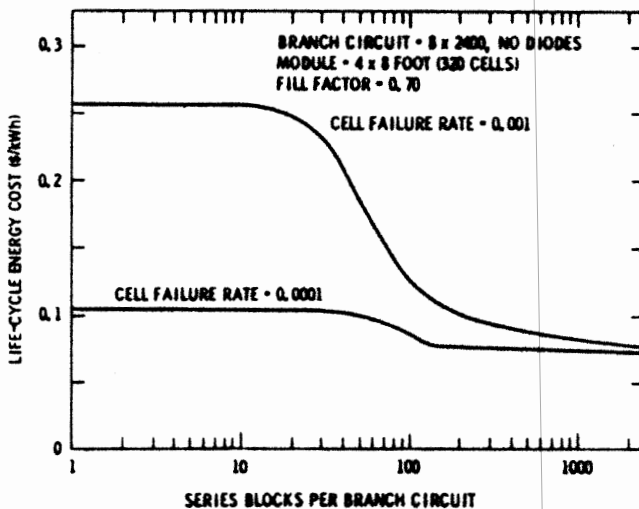


Fig. 8. Minimum life-cycle energy cost versus failure rate

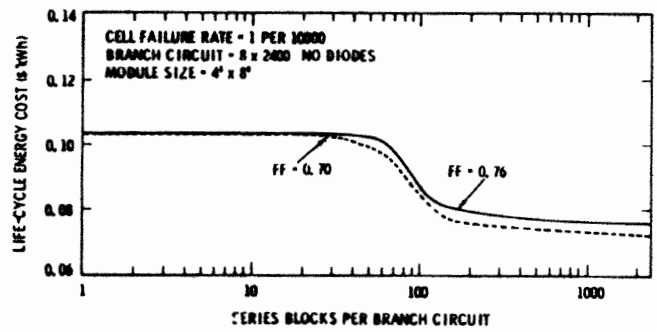


Fig. 9. Minimum life-cycle energy cost versus cell fill factor

Figure 9 illustrates another factor which can lead to faster than normal array degradation--cell or module fill factor. Higher fill factors cause the operating (maximum-power) current level to be closer to the array short-circuit current level. As a result, a reduction in current carrying capability due to a cell failure is more likely to lead to current limiting and reverse biasing with high-fill-factor cells and modules. The result is faster array degradation, and higher costs as shown in Figure 9.

Figure 10 expands the parametric study to include the effects of other choices for the number of parallel strings--in this case 4 and 16 strings in parallel. The number of parallel strings is found to have little influence on the overall conclusions relative to the optimum number of series blocks, the optimum module size, or the optimum maintenance strategy. As can be seen the primary effect is somewhat lower array degradation with correspondingly lower life-cycle energy costs for higher degrees of paralleling in the 100 series-block region of the plot. The higher degree of paralleling also has the advantage of minimizing hot-spot heating due to reverse-biasing effects.

As indicated in an earlier paper by this author, hot-spot heating increases with increasing numbers of series blocks (1). For present day solar cells with high shunt resistances the upper limit on the allowable number of series blocks is approximately 10 to 15. This in effect rules out the use of the

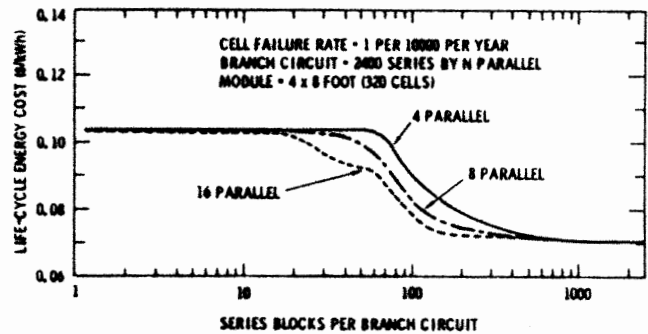


Fig. 10. Minimum life-cycle energy cost versus degree of paralleling

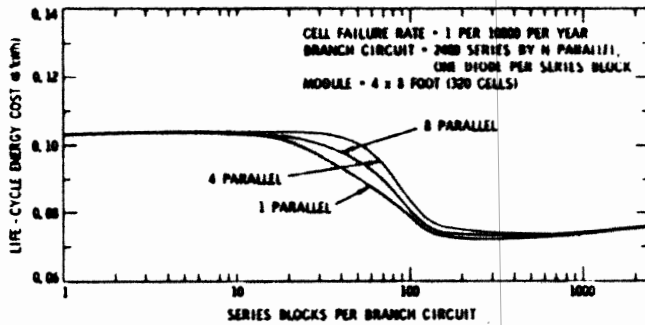


Fig. 11. Minimum life-cycle energy cost with by-pass diodes

large number of series blocks suggested by the earlier figures unless a corrective action such as by-pass diodes is incorporated into each branch circuit. This is indeed the recommended approach.

Figure 11 describes the life-cycle costs for a variety of branch circuit configurations incorporating a by-pass diode around each series block. Note that a single series string with diodes provides the least life-cycle cost followed closely by branch circuits with 8 or more parallel strings with diodes. To protect against hot-spot heating due to partial cell loss or shadowing, it is also desirable to limit the number of series cells per diode to 15 or less. For the example at hand with one diode per series block this further restriction requires that the number of series blocks be 160 or greater. The least life-cycle cost configuration which also maintains acceptable hot-spot heating levels is thus one with at least 160 series blocks and 160 by-pass diodes per branch circuit. A moderate degree of paralleling (8 or more) is useful to limit the total number of diodes required, and to achieve a reasonable number of branch circuits per power conditioner.

CONCLUSIONS

The approach of minimizing life-cycle cost over life-cycle energy has been shown to be a useful technique for array optimization, particularly when time-dependent parameters such as array degradation and maintenance are involved. The technique provides the necessary algorithm for integrating diverse attribute dependencies and drawing bottom-line conclusions relative to array

configuration tradeoffs. Data have been presented which show that the life-cycle cost for large ground-mounted arrays can be significantly reduced by selecting the optimum mechanical and electrical circuit configurations. Key factors include the incorporation of large modules to reduce support structure cost, and the incorporation of extensive series/paralleling and diodes to reduce module yield costs and eliminate the need for module field replacement.

REFERENCES

1. Ross, R. G., Jr., "Interface Design Considerations for Terrestrial Solar Cell Modules," Proceedings of the 12th IEEE Photovoltaics Specialists Conference, Baton Rouge, Louisiana, December 1976, pp. 801-806.
2. Gonzalez, C. and Weaver, R., "Circuit Design Considerations for Photovoltaic Modules and Systems," presented at the 14th IEEE Photovoltaics Specialists Conference, San Diego, California, January 7-10, 1980.
3. Bucciarelli, L. I., Jr., "Power Loss in Photovoltaic Arrays due to Mismatch in Cell Characteristics," *Solar Energy*, Vol. 23, 1979, pp. 277-288.
4. "Engineering Study of the Module/Array Interface for Large Terrestrial Photovoltaic Arrays," Final Report prepared for the Jet Propulsion Laboratory under contract number 954698, June 1977, Bechtel Corporation, San Francisco, California.
5. "Module/Array Interface Study," Final Report prepared for the Jet Propulsion Laboratory under contract number 954698, August 1978, Bechtel National, Inc., San Francisco, California.
6. Ross, R. G., Jr., "Photovoltaic Design Optimization for Terrestrial Applications," Proceedings of the 13th IEEE Photovoltaics Specialists Conference, Washington, D. C., June 5-8, 1978, pp. 1067-1073.
7. Nelder, J. A. and Mead, R., "A Simplex Method for Function Minimization," *Computer Journal*, Vol. 7, January 1965, pp. 308-313.